Grounding line migration of Petermann Gletscher, north Greenland, detected using satellite radar interferometry

Eric Rignot

Jet Propulsion Laboratory, California Institute of Technology, Pasadena 91109, California, U.S.A.

ABSTRACT Ice Sheet grounding lines are sensitive indicators of changes in ice thickness, sea level or elevation of the sea bed. Here, we use the synthetic-aperture radar interferometry technique to detect the migration of the limit of tidal flexing, or hinge line, of Petermann Gletscher, a major outlet glacier of north Greenland which develops an extensive floating tongue. Radar interferograms are generated over that glacier to measure its tidal deformation in response to ocean tide. The interferometric data are projected onto a common polar stereographic grid and co-registered to a reference radar scene with a precision of 5 m using the cross-correlation of the signal intensity. In each interferogram, the hinge line is mapped automatically with a precision of 30 m across the entire glacier width using a model fit from an elastic beam theory. The root-mean-square error of the model fit is less than 3 mm. Migration of the hinge line is subsequently detected with a precision of 40 m. Over periods of a few days to a few months, we observe a hinge line migration of 40 to 70 m which is due to changes in tide. 'J'he magnitude of the detected short-term migration is in good agreement with predictions made from tides calculated by the Grenoble global tide model combined wit h the glacier surface and bedrock slopes measured from laser altimetry and ice sounding radar data. Over the 3.87 years separating the 1992 and 1996 observations, the hinge line retreats 270± 120 m. The 120-m standard deviation shows that spatial variations in hinge line migration are significant, probably the result of subtle variations in bedrock topography. Expressed in terms of changes in ice thickness, the retreat suggests glacier thinning at a rate of 79±35 cm/yr ice volume equivalent. Coincidentally, an analysis

of the ice volume flux of Petermann Gletscher suggests that its ice flux at the hinge line exceeds its balance ice volume flux by $0.88 \pm 1 \mathrm{km}^3/\mathrm{yr}$, which suggests glacier thinning at a rate of 88+100 cm/yr. Hence, both the analysis of volume fluxes and the detection of a hinge line migration concur to suggest that Petermann Gletscher is currently loosing mass to the ocean.

INTRODUCTION

The transition region between the grounded part of an ice sheet and its floating part, often referred to as the grounding line, is fundamental to the stability of an ice sheet (Thomas and Bentley, 1978; Hughes, 1977; Weertman, 1974)). Because the glacier slopes are typically small at the grounding line, the position of the grounding line is sensitive to changes in ice thickness, sea level or elevation of the sea bed (Thomas, 1979; Hughes, 1977).

Locating a glacier grounding line in the field, or using remote sensing techniques, has however remained a challenging exercise (e.g. Vaughan, 1994). As a result, the grounding line of glaciers in the Antarctic or in Greenland are known with considerable uncertainty.

Synthetic-aperture radar interferometry is a new technique for measuring glacier deformation from space at the millimeter level over a period of just a few days (Goldstein and others, 1993). Over floating tongues and ice shelves, the measured glacier deformation is a combination of creep flow and tidal motion which can be separated using multiple interferograms (Hartl and others, 1994). Using this technique, the limit of tidal flexing of the glacier, or hinge line, may be measured at an unprecedented level of spatial detail and accuracy, simultaneously across the entire glacier width and with a uniform sampling scheme over large areas (Rignot, 1996; Rignot and others, 1997; Rignot, 1997).

Satellite radar interferometry is used here to reline our previous mapping of the grounding line of Petermann Gletscher, a major outlet glacier of north Greenland, and detect migration of its hinge line over a 4-year time period. The radar data were collected by the European Space Agency (ESA)'s Earth Remote Sensing Satellites (ERS- 1 and ERS-2) instruments. The mapping of the hinge line is repeated at different epochs and at different tide to separate the effect of snort term variations in sea level (tides) from that of a longer-term changes in glacier thickness. We analyze the errors associated with the mapping of the hinge line

and the detection of a hinge line migration. The inferred change in glacier thickness is then compared to an independent analysis of ice volume fluxes of Petermann Gletscher to conclude on its current state of mass balance and stability.

STUDY AREA

Petermann Gletscher, located at 60° W and 810 N on the northwestern flank of the Greenland Ice Sheet, is named after the famous German geographer Dr. A. Petermann (Koch, 1928). Petermann Fjord was discovered on August 27th, 1871 by Hall's U.S. Steamer Polaris expedition (Bessel, 1876), but it was not until June 1876 that Coppinger and Fulford realized that the fjord was filled with a glacier. in 1892, Pear-y discovered that the glacier was reaching far into the Inland Ice (Koch, 1940).

Petermann Gletscher is one of the longest glacier in the northern hemisphere. The glacier develops an extensive floating tongue (70-km long), with a terminus only a few meters above sea-level. In 1917, Koch (1928) noted that the outermost portion the glacier beyond a line drawn between Cape Agnes (where Porsild Gletscher meets with Petermann Gletscher) and Cape Coppinger was afloat, with a smooth surface free from crevasses (see Figure 1). The glacier grounding line is more or less in the same position today (Rignot, 1996). Similarly, historical photographs suggest that little change occurred in the glacier ice front position in the past 50 years (Higgins, 1991).

Although the historical record is suggestive of glacier stability, Petermann Gletscher is far from being a sluggish glacier (Weidick, 1995). It flows at more than 1km/yr into the Arctic ocean (Higgins, 1991), much faster than its immediate neighbors Humboldt Gletscher and Ryder Gletscher, and faster than any other glacier in north Greenland. It is by far the largest discharger of ice in north Greenland (Rignot and others, 1997). Like most other large outlet glaciers in the north, Petermann Gletscher looses mass to the ocean mostly

through basal melting of its floating tongue. Yet, nowhere in the north of and northeast sectors of Greenland are the inferred basal melt rates higher than on Petermann Gletscher (Rignot and others, 1997). How the glacier can maintain in mass balance while at the same time flow rapidly to the ocean and sustain massive removal of ice from basal melting remains unclear.

METHODS

Interferogram generation

The details of the method used to generate radar interferograms of Petermann Gletscher were described in Rignot (1996). in brief, we combine two passages of the ERS satellite coherently to form a radar interferogram, which is then corrected for surface topography using a prior-determined precision digital elevation model (DEM) of north Greenland assembled by Ekholm (1996). DEM control points are also used to refine the initial estimates of the orbit separation between the successive passages of the satellite (the so-called interferometric baseline) obtained from the ERS precise orbit data distributed by the German Archive and Processing Facility (DPAF).

Two topography-corrected interferograms spanning the same time interval are then differenced to yield an interferogram which measures only the surface deformation associated with the tidal motion of the glacier. We refer to this difference interferogram as a "tide interferogram " in the remainder of this paper. The success of differencing relies on the assumption that the glacier creep flow remains steady and continuous during the period of observation so that the deformation signal associated with creep flow be the same in both topography-corrected interferograms and cancels out when computing the difference. Where this assumption is unvalid, deformation fringes are found on grounded ice, as for instance in the case of the mini-surge of Ryder Gletscher (Joughin and others, 1997).

A single ERS interferogram measures the difference in tidal motion of the glacier in between two epochs. A double-difference or tide interferogram measures a quadruple difference in tidal deformation of the glacier (Rignot, 1996). In 1992, ERS repeated the same orbit every 3 days. Hence, the 1992 tide interferograms measure quadruple differences in tidal motion over 3-day periods. In 1996, ERS-1 and ERS-2 repeated the same orbit every 35 days but with ERS-2 trailing ERS-1 by one day. Tide interferograms formed by combining the signal from ERS-1 and ERS-2 thereby measure quadruple changes in tidal motion over one-day periods.

A consequence of the difference in repeat cycle of the 1992 and 1996 data is that the magnitude of the tidal deformation signal measured in the 1996 data is typically 2-3 times larger than that measured in the 1992 data. The reason is that the one-day repeat cycle of the 1996 data is closer to the natural cycle of diurnal and semi-diurnal tides than the 3-day repeat cycle of the 1992 data. Additional details on the ERS data used in the study, along with tide predictions made at the time of passage of the satellite, are given in Table 1.

Comparison of image products

To compare tide interferograms acquired at different epochs and possibly along slightly different orbits, the data are first projected onto a common Earth-fixed grid, here a polar stereographic (PS) grid, with a secant plane at 70 degrees north, and a 50-m sample spacing (Figure 1). The 50-m sample spacing is a conservative value since it is more than twice the natural sample spacing of the ERS data (20 m on the ground in the cross-track (or range) direction, and 4 m in the along-track (or azimuth) direction).

After projection onto the PS grid, the multi-date ERS data do not overlap perfectly due to uncertainties in absolute positioning of the radar images. The residual offsets between the data, typically about 1-2 pixels or 100 m, need to be estimated with precision in order to

minimize their effect on the precision of detection of a hinge line migration. Using one scene as a the reference radar scene, the residual offsets are estimated using the cross-correlation of the radar signal intensity. The offsets are calculated on a regular grid (excluding areas of glacier flow to avoid unnecessary biases in the registration), filtered based on the signal-to-noise ratio of the correlation peak (offsets with a high noise level are thrown out) and least-square fitted through a plane. The root-mean-square error (rms) of the plane fitting is typically less than 0.1 sample spacing or 5 m for the three precision registrations required for this study. This means that the multi-date data are co-registered with a precision of 5 m. Although that number may seem presumptuous to the reader unfamiliar with radar remote sensing, co-registration accuracies of the order of several decimeters are commonly achieved in radar interferometry applications using a similar approach.

The registered tide interferograms, centered about the hinge line of Petermann Gletscher, are shown in Figure 2. The hinge line is located at the inward limit of the zone of tidal flexing or flexure zone. The flexure zone is a region about 4-6 km in length, of high fringe rate in Figure 2, where the glacier adjusts rapidly to hydrostatic equilibrium as it reaches the ocean.

Systematic mapping of the hinge line

In a prior study of Petermann Gletscher, the glacier hinge line was mapped by locating the minimum of one-dimensional tidal profiles successively across the entire glacier width (Rignot, 1996). While this earlier procedure was sufficient to locate the hinge line for mass flux calculations, it is not optimal for change detection applications. Here, we improved upon tile mapping precision of the hinge line by using a model fitting technique (Rignot, 1997). Instead of using a few points to locate the hinge line, the method uses entire profiles and is therefore more! robust to noise.

The predicted flexure of an elastic beam, $w(x)$, is written as

$$w(x) = \frac{(w_{max} - w_{min})}{(1 + exp(-\pi))} [1. - exp(-\beta(x - x_H))][\cos(\beta(x - x_H)) + \sin(\beta(x - x_H))], x > x_H \quad (1)$$

$$w(x) = 0, x < x_H$$

where β is the flexural rigidity of the ice (m^{-1}), x is the abscissa along the profile (m), and $x = x_H$ at the hinge line. For each tidal profile, we estimate 4 parameters in the least-square sense: the flexural rigidity of the ice, β, the maximum and minimum height of the profile w_{max} and w_{min}, and the position of the hinge line x_H. A measure of the goodness of fit is provided by the r.m.s. difference between the model and the interferometric data. The hinge line migration is then detected as the shift in position of x_H along the profile in between two epochs.

An example of model fitting is shown in Figure 3a-b. Over the more than 1,000 profiles analyzed in this study, the goodness of fit is 3 ± 1 mm on average. At this level of precision, one can hardly notice the difference between model fit and real data, which illustrates both the low noise level of the data and the relevance of the elastic model.

Model fitting is less reliable along the side margins (Figure 2). This is expected because the glacier tidal deformation in that region is the result of complex interactions between the glacier grounding line, the side margin grounding line, and the grounding line of Porsild Gletscher (Figure 1). A consequence of this interaction is a "pinching" of the zone of tidal flexure along the side margins which cannot be accounted for by a simple one-dimensional elastic beam model. Similarly, the inferred values of flexural rigidity of the ice become less realistic along the glacier side margins compared to the glacier center.

To estimate the mapping precision of the hinge line, we smoothed the inferred hinge line profile using a square box averaging filter about one ice thickness in width (or 600 m) and compared the resulting profile to the original profile. The rms of the difference is 30 m

on average. This value represents the statistical noise of our relative determination of the position of the hinge line at one epoch.

Using the same approach, we estimated the precision with which a hinge line migration is detected. On average, the standard deviation of the difference between twop profiles over an area about one ice thickness in width is 40 m. This value is consistent with the abovementioned mapping precision of the hinge line assuming that the hinge line profiles are all mathematically independent.

The abovementioned mapping precision is a relative number which defines how well the hinge line may be mapped in reference to the radar data. It does not define the absolute position of the hinge line on a cartographic reference. In the absence of ground control points of known geolocation, the absolute precision of mapping of the hinge line is probably no better than 100 m since we referenced the data to a DEM (Ekholm, 1996) which has a natural sample spacing of 500 m and data co-registration to the DEM has a typical noise level of about ± 0.1 DEM sample spacing. Although this factor may appear as a limitation of the technique when compared for instance to the results of Global Positioning System (GPS) surveys which can be absolutely referenced ground surveys to within 5-1o m, it is important to note that the uncertainty in absolute location of the radar data has no influence on the precision of detection of a hinge line migration from the same radar instrument.

No other measurements of the location of the hinge line are available on Petermann Gletscher to compare our results with a ground reference. laser altimetry data and ice sounding radar data can locate the grounding line within a few hundred meters to a kilometer at best. Similarly, GPS data collected on Rutford Ice Stream, Antarctica exhibit a rms noise one order of magnitude larger (cm) than that achieved with ERS radar interferometry (mm) (Rignot, 1997), with the result that the hinge line may only be mapped with a precision of 100-200 m (Vaughan, 1994) compared to several tens of meters with radar interferometry.

Simply stated, the precision of mapping of the hinge line achieved with radar interferometry is totally unprecedented.

RESULTS

Hinge line migration

Four independent mappings of the hinge line of Petermann Gletscher are shown in Figure 4. Two main features may be identified from the inferred profiles: 1) the hinge line migrates back and forth on a short term basis both in 1992 and 1996, which we interpret as the result of changes in tide; 2) the hinge line retreats on average several hundred meters between 1992 and 1996, presumably due to a change in glacier thickness.

The hinge line migration is 78+213 m between the two 1992 interferograrns and 42+162 m between the two 1996 interferograms (where ± denotes the value of the standard deviation of the difference). The magnitude of this migration is above the statistical noise of our data. It indicates that on a short term basis the grounding line of Petermann Gletscher migrates back and forth within a 100-m region. Along the glacier side-margins, the short-term variability in position of the hinge line is possibly larger (several hundred meters), as suggested by a comparison of the interferograms in Figure 2 and the tidal profiles shown in Figure 4. The mapping precision is also less in that region.

This first result indicates that the transition from grounded to floating ice is not a uniform grounding line, but rather a "grounding zone" which extends several tens of meters in length at the glacier center and possibly several hundred meters along the glacier side margins. As discussed in the next section, the detected 40-80 m short-term variation in position of the hinge line may be completely explained by changes in tide.

The hinge line retreat measured between 1992 and 1996 from individual profiles varies from

212±230 m (1992 minus 1996bis) to 333±127 (1992bis minus 1996). After averaging of the two 1992 profiles and the two 1996 profiles (thick curves in Figure 4), we obtain an average hinge line ret rest of 272+120 m. The standard deviation of the difference is less than in the comparison of individual profiles, which means that the effect of a short-term variability in position of the hinge line due to tide is effectively averaged out when two independent profiles are averaged together, but interestingly the mean value of the retreat remains within ±50 m of that inferred from individual profiles.

The glacier slope of Petermann Gletscher at the hinge line may be deduced from the glacier elevation profile collected by the NASA/Wallops airborne laser altimeter (Krabill and others, 1995) combined with ice thickness data collected also in 1995 by the University of Kansas' ice sounding radar (ISR) (Allen and others, 1997). The surface slope along the profile is 1 percent at the hinge line, and the inferred bedrock slope is also 1 percent (Figure 5). The KMS DEM also indicates a 1 percent glacier slope at the hinge line.

The ice thickness change, δh, corresponding to a hinge line migration, δx_H, is given by (Thomas and Bentley, 1978)

$$\delta h = \delta x_H \left[\left(1. - \frac{\rho_w}{\rho_i}\right)\beta - \alpha\right] \qquad (2)$$

where ρ_w is the density of sea water, pi is the column-averaged density of ice, β is the bedrock slope counted positive downwards, and α is the surface slope counted positive upwards.

Using ρ_w=1030 kg m^{-3} and ρ_i=917 kg m^{-3}, we find that the hinge line retreat of 272±120 m measured between 1992 and 1996 (the mean time difference between the two mappings is 3.87 years according to Table 1) corresponds to a glacier thinning rate of 79±35 cm/yr.

Comparison with predicted tides

Tidal predictions at the time of passage of the ERS satellite were made using the Grenoble finite element ocean tide model FES95.2 which predicts the 8 major tidal constituents (3 diurnals (Kl, 01, Q]), and 5 semi-diurnals (M2, S2, N2, K2, 2N2) on a 0.5 x 0.5 degree regular grid (Le Provost and others, 1997). The 4 major constituents (M2, K2, 01 and S1) predicted at the location of Thank God Harbor (north of Petermann Gletscher front) were compared to that measured by the U.S. 'Polaris' expedition in 1871 (Bessel, 1876). The root mean square error of the predicted constituents is 1.7 cm, which is consistent with the estimated global precision of 2.8 cm derived by Le Provost and others (1997). Hence, the ocean tides predicted by the tide model should be accurate to within a few centimeters.

The predicted tides for Petermann Gletscher (latitude = 81.5 north, longitude = 63 deg. west) at the time of passage of the ERS satellite are listed in Table 1. Comparison of these data with the tidal amplitudes measured in the ERS tide interferograms is shown in Table 2. The difference between predicted tidal differences and those measured by ERS is 1.5 cm on average, wit h a standard deviation of 3.6 cm. The agreement between model prediction and measured tides is remarkable given that the model solution does not include the detailed geometric characteristics of Petermann Fjord and is made for an area about 80 km north of the hinge line, at the mouth of Petermann Fjord, in Hall Basin. The result confirms both the relevance of the tidal model and the precision of the interferometric measurements of tidal differences.

Tide predictions are very useful to interpret the interferometric measurements. Radar interferometry only measures changes in tidal deformation and hence does not provide any information on absolute tide. As the tide changes, the glacier hinge line is expected to migrate back and forth to maintain hydrostatic equilibrium. In the case of the sea bed geometry shown in Figure 5, the hinge line will migrate inward for positive tides and seaward

for negative tides. If the tidal amplitude is known, however, as well as the glacier slopes, it is conceptually possible to remove the bias in location of the hinge line introduced by tide to recover the longer-term average position of the hinge line.

A simple first-order analysis of Eq. (1) in the proximity of $x = x_H$ reveals that the hinge line position corresponding to the difference between one profile for which the hinge line is at $x = x_{H1}$ and another for which the hinge line is at $x = x_{H2}$ yields an intermediate position of the hinge line at $(x_{H1} + 2_{H2})/2$. The result is valid to first order as long as x_{H1} and x_{H2} remain in the proximity Of the average position x_H, which means that $\beta(x_{H1} - x_{H2})$ is small compared to one or that the hinge line does not migrate by more than a kilometer. The analysis also reveals that tidal deformation signal will be recorded inward of the hinge line $(x_{H1} + x_{H2})/2$, up to the minimum value of x_{H1} and x_{H2} along the x-axis. We draw two conclusions from these observations: 1) a tide interferogram assembled from ERS data will yield an average position of the hinge line in between 4 epochs, hence a position of the hinge line which is less affected by tide than if the radar were measuring "instantaneous" tides; and 2) residual tidal deformation signal may still exist inward of the detected hinge line, and the inward extent of this deformation signal will depend on the largest positive tide experienced by the glacier at the time of satellite imaging.

Using the calculated tides at the ice front of Petermann Gletscher, we predicted the effect of tide on its hinge line migration and compared the results with the ERS data. We find that in 1992, the hinge line should have migrated 50 m on average across the glacier width versus 78 m measured (the sign of migration is correctly predicted). In 1996, the hinge line should have migrated 56 m on average versus 42 m measured. The difference between calculated and real migration is within the noise level of our data. We conclude that the short-term variation in hinge line position is associated with changes in tide.

Analysis of Mass fluxes

The hinge line flux of Petermann Gletscher is 12.0 ± 0.5 km^3/yr ice volume equivalent (Rignot, 1996). The ice volume flux measured at the glacier equilibrium line elevation is 12.4 km^3/yr (Joughin, pers. comm., 1997). The location of these two profiles is shown in Figure 1. In between the two profiles the glacier looses mass through surface ablation, and accumulates mass from snow fall.

We calculated surface ablation in between the two profiles using Reeh's (1991) degree day model. A degree day factor of 9.8 mm/deg/day was implemented since this is the value measured by past experiments conducted in northern Greenland (9.6 mm/deg/day on Storstrømmen Gletscher in the northeast measured by Bøggild and others (1994); 9.8 and 5.9 mm/deg/day measured by Braithwaite and others (1997) at two sites near the Hans Tausen Ice cap in north Greenland; and 9.8 mm/deg/day in Kronprins Christian Land measured by Konzelmann and Braithwaite, 1995). The degree day factor of 8 mm/deg/day commonly used by ice sheet modellers in the remained of Greenland, and which is based on in-situ ablation studies conducted at lower latitudes along the west coast, underpredicts ablation in the north, as first pointed out by Braithwaite (1995). More recently, Van de Wal (1996) compared predictions from an energy balance model and the degree day model of Reeh (1991) with an 8 mm/deg/day degree day factor and concluded that the degree day model significantly underestimates ablation in the north. If Van de Wal's model predictions were correct, Peterrnann Gletscher mass imbalance quoted in this study as well as in Rignot and others (1997) would be larger. We however chose to use the degree day model because it depends mostly on one parameter, the air temperature, whereas the energy balance model depends on a lot of parameters more difficult to parametrize.

Mass accumulation was computed from Ohmura and Reeh (1991) regridded from the original ice core data courtesy of Fahnestock and Joughin (pers. comm., 1996). The result for the

1056 km^2 area in between the two profiles (excluding ice feeding into the main glacier flow from the sides) is a surface ablation of 1.42 km^3/yr and a mass accumulation of 0.28 km^3/yr. The net result is a balance ice volume flux at the hinge line of 11.2 km^3/yr.

Total mass accumulation of Petermann Gletscher above the grounding line is 13.1 km^3/yr, and surface ablation is 2.0 km^3/yr. The balance ice flux at the hinge line should therefore be 11.1 km^3/yr (Rignot and others, 1997), similar to the value calculated above based on a comparison with the ice flux at the equilibrium line elevation. This means that: 1) the ELA ice flux is in balance with mass accumulation in the interior, as first observed by Joughin (pers. comm. 1996); and 2) the measured hinge line ice volume flux is larger than that estimated to maintain Petermann Gletscher in a state of mass balance.

The uncertainty in mass accumulation is 10 percent based on the fact that the shallow ice core data of Ohmura and Reeh (1991) indicate a mass accumulation which may be 10 percent in error compared to the long-term average. Spatial sampling of ice cores in the north is however poor compared to other parts of Greenland, which means that the uncertainty in mass accumulation could actually be greater than 10 percent.

Surface ablation may be in error depending on the quality and resolution of the DEM utilized to parametrize the air-temperature, Our predictions should be little affected by the quality of the DEM, however, since we use the precision KMS DEM of north Greenland assembled at a 500-m spacing with a vertical precision of about 10 meters on ice (Ekholm, 1996). The parametrization of the air-temperature is probably subject to more significant uncertainties and the degree day factor may vary from one glacier to the next. We estimate that our surface ablation numbers should be accurate to the 10-percent level (although errors as large as 20 percent cannot be excluded on a glacier per glacier basis), resulting in an overall uncertainty in balance flux of 14 percent.

If the above estimates are correct, the hinge line ice flux of Petermann Gletscher exceeds its balance ice volume flux by $0.88 \pm 1. km^3/yr$. This means in turn that Petermann Gletscher looses mass to the ocean. The inferred rate of ice thinning averaged over the entire area between the ELA and the grounding line is 88 ± 100 cm/yr.

Although the above result is affected by a large error due to uncertainties in ablation and accumulation, the trend suggested by the ice volume flux method is consistent with the more precise estimate obtained from the hinge line retreat. Both methods concur to indicate that Petermann Gletscher is currently thinning at a rate of about 80 ± 35 cm/yr. Taken differently, this could also mean that our estimates of mass accumulation and ablation on Petermann Gletscher are not far from the actual truth.

If the ice volume fluxes are correct, it indicates that Petermann Gletscher mass imbalance is concentrated at the coast. It also means that it would be dangerous to conclude that Petermann Gletscher is in balance based solely on a comparison of its ice volume flux at the ELA with mass accumulation in the interior. The comparison of ice fluxes should be done at the coast, if the overall objective of the study is to measure the contribution of this portion of the ice sheet to sea-level rise. To improve the quality of the estimates of the balance flux, in-situ studies are necessary to characterize surface ablation better. Similarly, more ice core data are needed in the north. The net advantage of the hinge line method in that regard that it is independent of our knowledge of mass accumulation in the interior and mass ablation at the coast. Until more in-situ data on accumulation and ablation are collected in the north, detecting the hinge line migration of outlet glaciers may be the most effective way to complement the measurements of ice volume changes to be conducted by laser altimetry systems over the next decades.

CONCLUSIONS

This study demonstrates the feasibility of using radar interferometry to detect the hinge line migration of a large outlet glacier from space, and thereby gather precise information on its state of balance and stability, independent of our knowledge of mass accumulation and surface ablation. in general, multiple independent mappings of the hinge line will be necessary to separate the effect of short term changes in sea level induced by tide from longer-term changes in glacier thickness. Where tidal predictions are available from a tide model, however, the requirement on the number of radar scenes needed to achieve a certain level of precision may be relaxed as the tide predictions may help remove the uncertainty in location of the hinge line associated with tide. Of course, the method requires information on the glacier surface and bedrock slopes, which can be obtained from laser/radar altimetry and ice sounding radars. Radar altimetry data are now available over the whole of Greenland and Antarctica.

On Petermann Gletscher, the radar interferometry technique is capable of locating the hinge line with a precision of 30 m, and detect a hinge line migration with a precision of 40 m. This level of precision is totally unprecedented, and beyond the capabilities of in-situ techniques such as GPS. When repeated across the entire glacier width, the approach shows that the hinge line migration is not a clear moving front but rather a “grounding zone” with significant spatial variability over a region typically 100-m wide. This variability is above the noise level of the data, therefore real, and probably associated with subtle variations in bedrock topography. This situation may be typical of most tidal glaciers. A consequence of this spatial variability is that it is probably essential to map the hinge line across the entire glacier width (instead of a couple profiles) and at different epochs before any conclusions may be reached regarding the status of advance/retreat of the hinge line. This type of mapping is uniquely addressed by satellite techniques.

On Petermann Gletscher, both the mass flux method and the detection of a hinge line migration concur to suggest ice thinning, with the hinge line migration method offering greater precision in the measurement of ice thinning. What the remote sensing techniques do not explain, however, is the exact cause of ice thinning on Petermann Gletscher. Over one century, a 79-cm/yr glacier thinning should have resulted in a significant retreat of the 70-m thick glacier front, which does not seem to be the case. Hence, we hypothesized that the retreat may be a recent phenomena. The mass flux method suggests that the mass loss is concentrated at the coast, because the glacier flows too fast. More information on the ablation characteristics of the glacier, both above (surface) and below (basal) are urgently needed.

ACKNOWLEDGEMENTS. This work was performed at the Jet Propulsion Laboratory, California Institute of Technology, under a contract with the National Aeronautics and Space Administration, Polar Program. We thank Robert Thomas for useful discussions about this study, Prasad Gogineni for providing the ice sounding radar observations of Petermann Gletscher, William Krabill for providing the laser altimetry data of Petermann Gletscher, and Simon Ekholm for continuous use, development and distribution of his digital elevation model of north Greenland. We also thank the European Space Agency for kindly providing the ERS radar data through a very professional and helpful staff organization.

REFERENCES

Allen, C., S. Gogineni, B. Wohletz, K. Jezek and 1'. Chuah. 1997. Airborne radio echo sounding of outlet glaciers in Greenland, *Int. J. Rem. Sens.* 18(14), 3103-3107.

Braithwaite, R.J. 1995. Positive degree-day factors for ablation on the Greenland ice sheet studied by energy-balance modelling. *J. Glaciol.* 41 (137), 153-160.

Braithwaite, R.J., T. Konzelmann, C. Marty and Ole B. Olesen. 1997, Errors in daily ablation measurements in North Greenland, 1993-94, and their implications for glacier-climate studies, *J. Glaciol.*, subm.

Braithwaite, R. J., '1'. Konzelmann, C. Marty and Ole B. Olesen. 1997. Reconnaissance study of glacier energy balance in North Greenland, 1993-1994. *J. Glaciol.*, subm.

Bøggild, C. E., N. Reeh, and H. Oerter. 1994. Modelling ablation and mass-balance sensitivity to climate change of Storstrømmen, Northeast Greenland, *Global and Planetary Change 9, 79-90.*

Bessel, E. 1876. Scientific results of the United States Arctic Expedition Steamer 'Polaris', C. F'. Hall commanding, Vol. 1 Physical Observations, Washington D.C.

Ekholm, S. 1996. A full coverage, high-resolution, topographic model of Greenland computed from a variety of digital elevation data. *J. Geophys. Res.* **101(B1O), 21,961--21,972.**

Goldstein, R. M., H. Engelhardt, B. Kamb and R.M. Frolich. 1993. Satellite radar interferometry for monitoring ice sheet motion: application to an Antarctic ice stream. Science, 262(5139), 1525-1530.

Hartl, P., K.H. Thiel, X. Wu, C. Doake and J. Sievers. 1994. Application of SAR interferometry with ERS-1 in the Antarctic. *Earth Observation Quarterly* 43, ESA Pub., 1-4.

Higgins, A. 1991. North Greenland glacier velocities and calf ice production. *Polar forschung, 60(1), 1-23.*

Holdsworth, G. 1969. Flexure of a floating ice tongue. *J. Glaciol., 8(54), 385-397.*

Holdsworth, G. 1977. Tidal interaction with ice shelves. *Ann. Geophys.*, 33(1/2), 133-146.

Hughes, T.J. 1977. West Antarctic ice streams, Rev. *Geophys. Space Phys.* **15(1), 1-46.**

Joughin, I., S. Tulaczyk, M. Fahnestock and R. K wok. 1996. A mini-surge on the Ryder glacier, Greenland, observed by satellite radar interferometry. *Science 274(5285), 228-230.*

Krabill, W. B., R.H. Thomas, C.F. Martin, R.N. Swift and E.B. Frederick. 1995. Accuracy

of airborne laser altimetry over the Greenland Ice Sheet, *Int. J. Rem. Sens.* **16(7), 1211-1222.**

Koch, L. **1928.** Contributions to the glaciology of North Greenland, *Medd. Grønland*, 65(2), 181-464.

Koch, L. **1940. Survey** of North Greenland, *Medd. Grønland, 130(1), 358* pp.

Konzelmann, T. and R.J. Braithwaite. 1995. Variations of ablation, albedo and energy balance at the margin of the Greenland Ice Sheet, Kronprins Christian Land, eastern North Greenland. *J. Glaciol.*, **41(137), 174-182.**

Le Provost, C., F. Lyard, J.M. Molines, M.L. Genco and F. Rabilloud, A Hydrodynamic Ocean Tide Model Improved by assimilating a satellite altimeter derived dataset. submitted to *J. Geophys. Res., 1996.*

Ohmura, A. and N. Reeh. 1991. New precipitation and accumulation maps for Greenland. *J. Glaciol.* **37(125), 140-148.**

Reeh, N. 1991. Parametrization of melt rate and surface temperature on the Greenland Ice Sheet. *Polarforschung* **59(3), 1989, 113-128.**

Rignot, E. 1996. Tidal flexure, ice velocities and ablation rates of Petermann Gletscher, Greenland, *J. Glaciol. 42(142), 476-485.*

Rignot, E. 1997. Radar interferometry detection of hinge line migration on Rutford Ice Stream and Carlson Inlet, Antarctica, *Ann. Glaciol.*, subm.

Rignot, E., S. P. Gogineni, W. B. Krabill and S. Ekholm. 1997. Ice discharge from north and northeast Greenland as observed from satellite radar interferometry, Science 276, 934–937.

Thomas, R.H. and C. R,. Bentley. 1978. A model for Holocene retreat of the west antarctic ice sheet, *Quarternary Research* **10(2), 15-170.**

Thomas, R.H. 1979. The dynamics of marine ice sheets, *J. Glaciol.* 24(90), 167-177.

Vaughan, D.G. 1994. Investigating tidal flexure on an ice shelf using kinematic GPS, *Ann. Glaciol. 20, 372-376.*

van de Wal, R.S.W. 1996. Mass-balance modelling of the Greenland Ice Sheet: a comparison of an energy-balance and a degree-day model. *Ann. Glaciol.*, 23, 36–45.

Weidick, A. 1995. Greenland. U.S. *Geol. Surv. Prof. Pap. 1386*, (Denver, CO, 1995), C1–C105.

Weertman, J. 1974, Stability of the junction of an ice sheet and an ice shelf, *J. Glaciol.*

13(67), 3--11.

Table 1. ERS-1 data used in this study and tides predicted at the time of passage of the satellite using the Grenoble tidal model (Le Provost and others, 1997). Each ERS-1 image acquired in 1995-1996 was combined with an ERS-2 image to form a radar interferogram. ERS-1 only images were combined in 1992. to form radar interferograrns.

ERS1 Orbit-(ERS2 Orbit-)Frame	Date(s) (MM-DD-YY)	Predicted Tide(s) (cm)
22373-2700-1953	25-10-9526-10-95	90.286.5
23876-4203-1953	07-02-9608-02-96	63.849.9
23332-3659-1953	31-12-9501-01-96	-10.37.5
23833-4160-1953	04-02-9605-02-96	71,474.3
2904-1953	04-02-92	73.3
2947-1953	07-02-92	52.0
2990-1953	10-02-92	4.2
3205-1953	25-02-92	-11.5
3248-1953	28-02-92	7.6
3291-1953	02-03-92	52.2

Table **2.** Comparison of measured tidal differences by ERS with that predicted from the FES.95.2 Grenoble tidal model (Le Provost and others, 1997).

ERS-1 Tide Interferogram	Tidal Difference Measured (cm)	Tidal Difference Predicted (cm)
22373-23876	-12.9	-10.2
23332-23833	-10.3	-14.9
2947-2904-2990	+30.9	+ 2 6 . 6
3248-3291-3205	-25.8	-25.5

Figure Captions

Figure 1. Radar amplitude image (140 x104 km), in a polar stereographic projection (50-m sample spacing), of Petermann Gletscher, North Greenland, acquired by ERS-1 on Dec. 31, 1995. The glacier flow to the north along the eastern flank of Washington Land. ISR1 denotes the Ice Sounding Radar data collected along the main ice flow (Allen and others, 1997) (Figure 5). ISR 2 denotes the ISR data collected in the transverse direction, approximately at the Equilibrium Line Altitude of the glacier. The hinge line profile inferred from the ERS interferometric data is shown as a thin white line, west of Porsild Gletscher. ERS was flying from left to right in the figure, illuminating from the botton (descending, right looking pass). ©ESA 1995

Figure 2. Tidal displacement and hinge line of Petermann Gletscher measured from ERS radar interferometry in (a) 1992 (3205-3248-3291 in Table 1-2); (b) 1992bis (2904-2947-2990 in Table 1-2); (c) 1996 (23332-23833 in Table 1-2) and (d) 1996bis (22373-23876 in 'I'able 1-2) (Table 1 and 2). Each fringe or full cycle of grey tone variation represents a 28-mm differential displacement of the glacier tongue along the radar line of sight - equivalent to a 31-mm vertical displacement of the glacier tongue - induced by changes in ocean tide. The location of profile PI in Figure 3 is indicated in the upper left quadrant (white thick line), 1992, and is parallel to the lSR 1 profile shown in Figure 1.

Figure 3. (a) Tidal profile PI (Figure 2) measured interferometrically by ERS (dots) and model fit from an elastic beam theory (solid line) and (b) difference between the model and the ERS data. The rms error of the model fit is 1.7 mm. The inferred flexural rigidity of the ice is $\beta = 0.3\ \mathrm{km}^{-1}$. The inferred location of the hinge line is indicated by an arrow in panel (a).

Figure 4. Hinge line migration of Petermann Gletscher between four different epochs (Table 1-2) inferred from model fitting of tidal profiles (Figure 2). (a) Thin lines shows the hinge line position in 1992 and 1992bis (black lines), and 1996 and 1996bis (grey lines). Thick curves show the average profile in 1992 (black thick line) and 1996 (grey thick line). (b) Hinge line retreat between the 1992 and 1996 average profiles.

Figure 5. Thickness profile of Petermann Gletscher, north Greenland, based on 1995 laser altimetry data for the surface (Krabill and others, 1995) and ice sounding radar data for the thickness (Allen and others, 1997). The precision in surface elevation is 10 cm, and 10 m for the ice thickness. The position of the hinge line inferred from radar interferometry in late 1995 is indicated by an arrow. The grounding line and the line of first hydrostatic equilibrium of the ice are 1-2 km below the hinge line (Rignot and others, 1997). The glacier surface and bedrock slopes, shown by the IO-km long solid line fits, are 1 ± 0.1 percent.

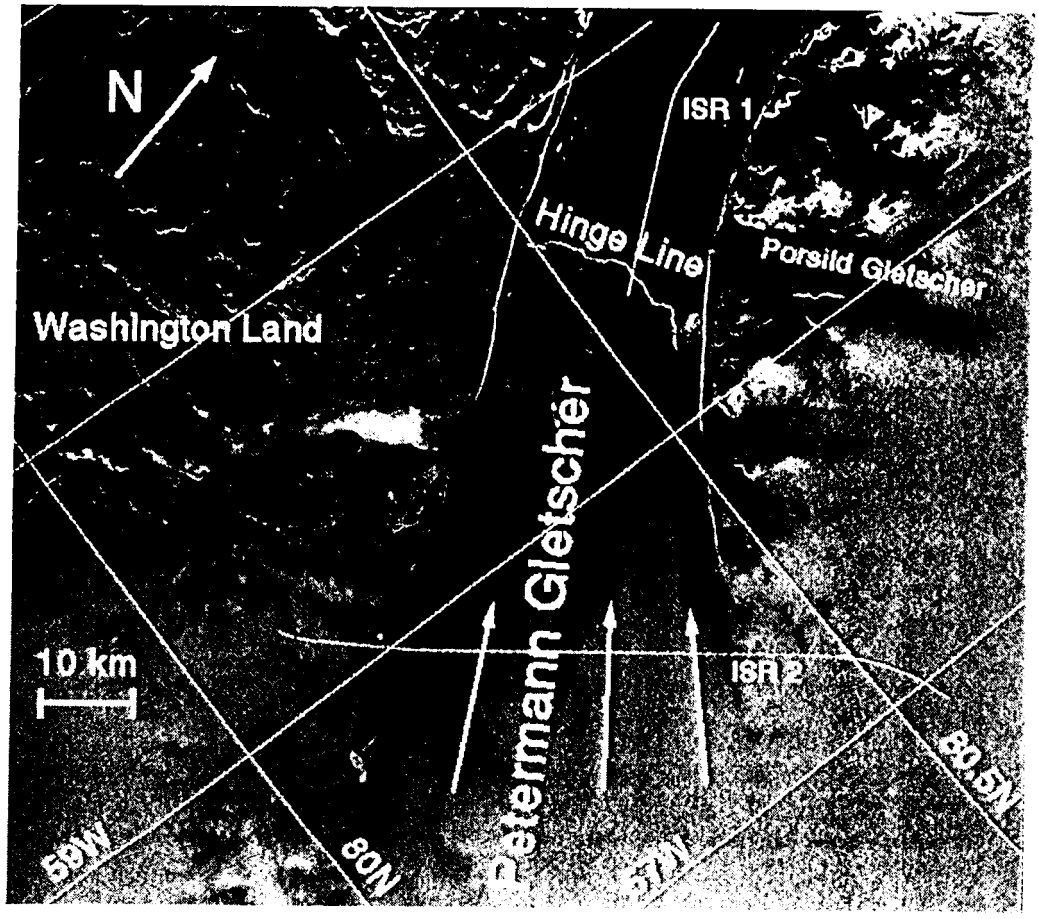
N
ISR 1
Hinge Line
Porsild Gletscher
Washington Land
Petermann Gletscher
10 km
ISR 2
59W
80N
80.5N

Figure 1.

(a) (b)

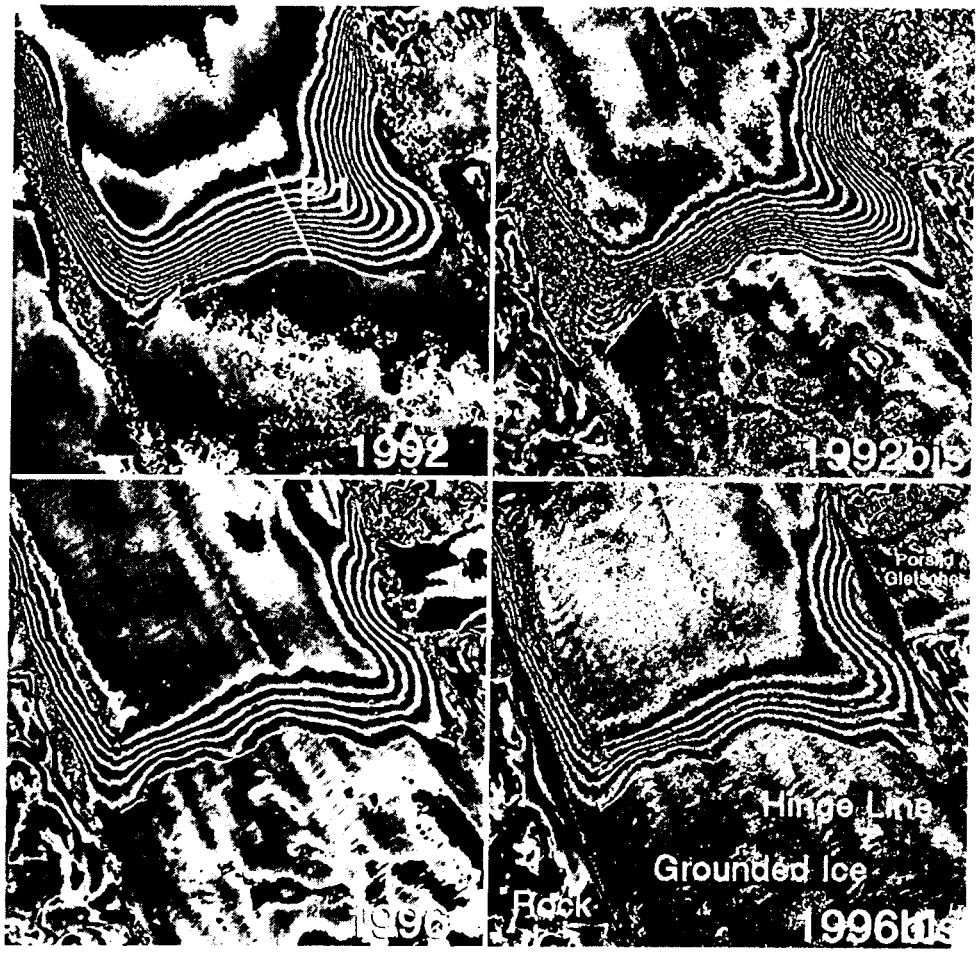

Figure 2

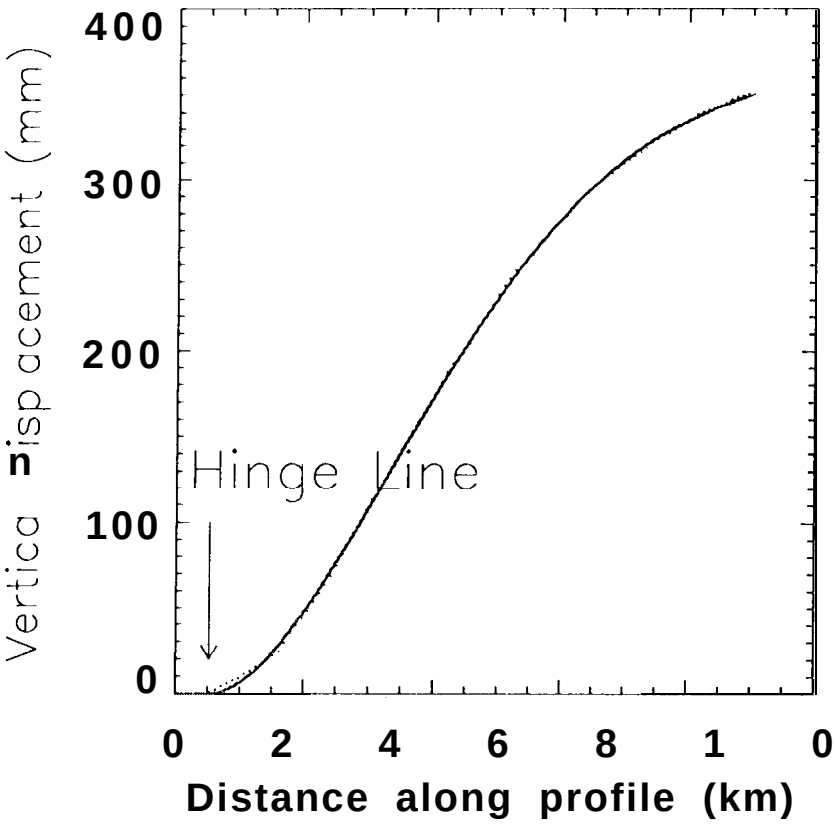
400
300
200
100
0
Vertica nisp acement (mm)
Hinge Line
0 2 4 6 8 1 0
Distance along profile (km)

(a)

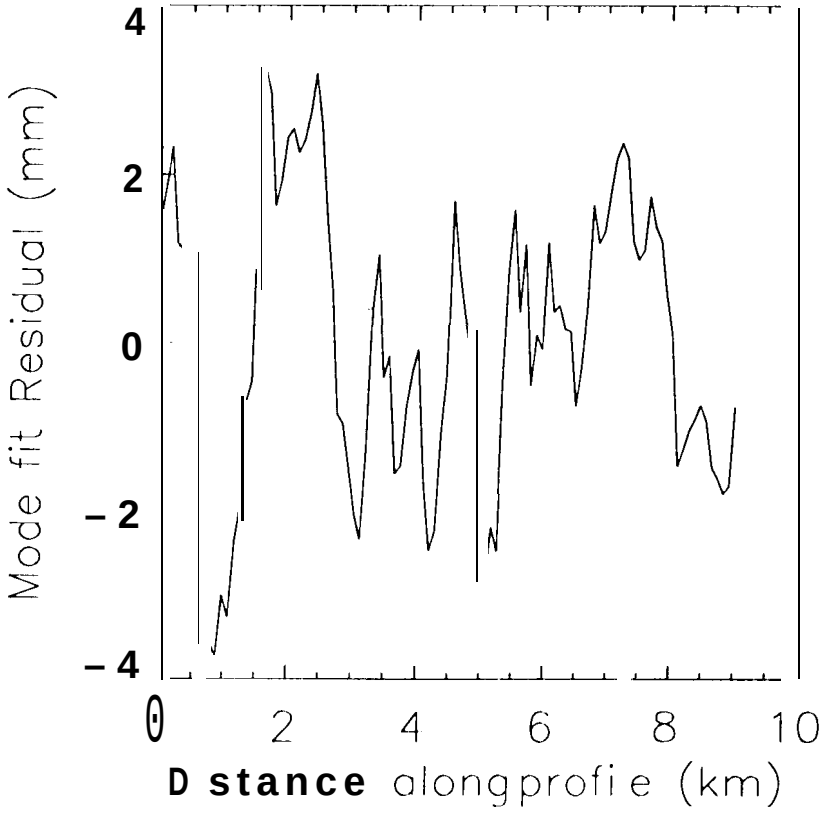
4
2
0
– 2
– 4
Mode fit Residual (mm)
0 2 4 6 8 10
D stance alongprofi e (km)

(b)

Figure 3

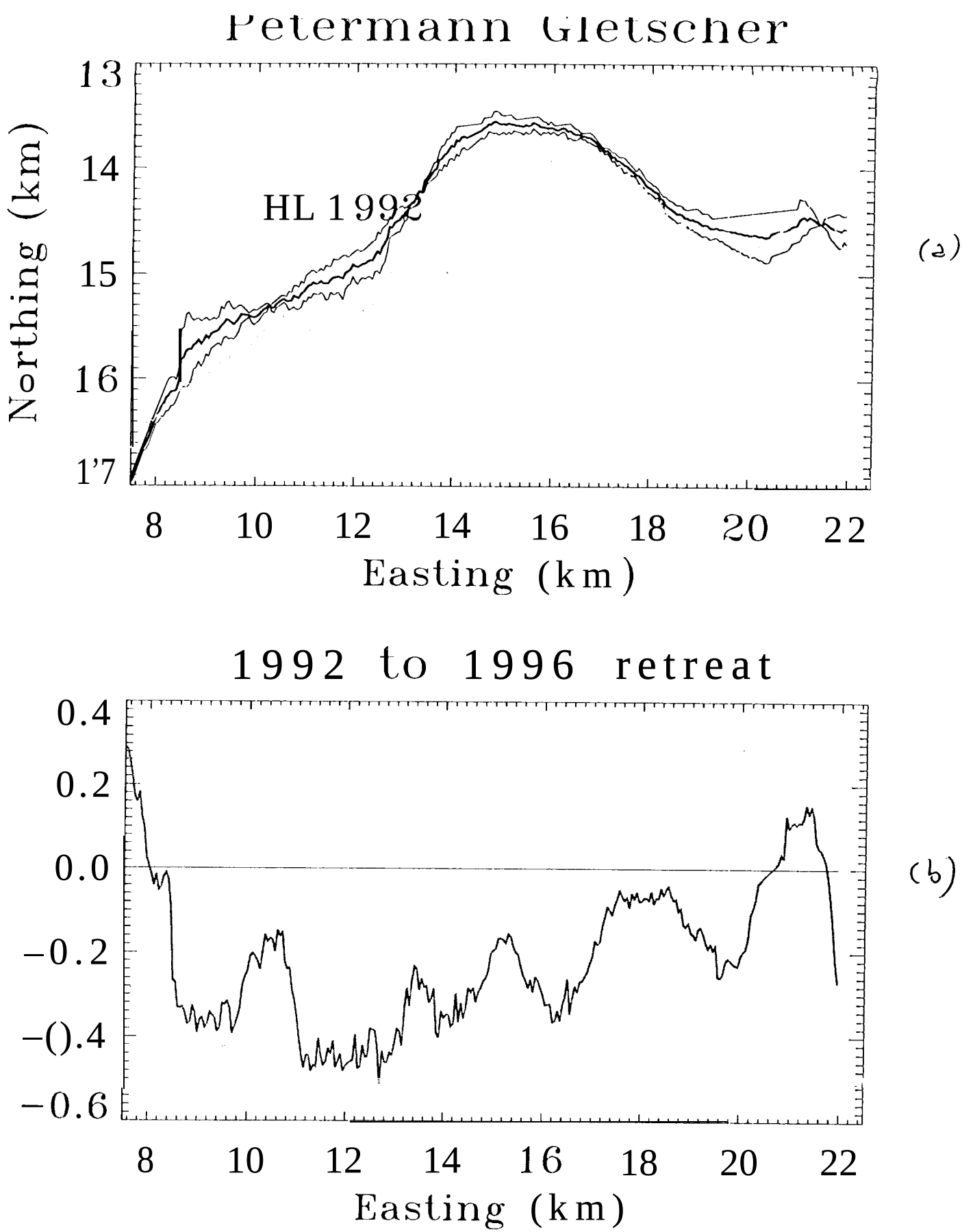
Petermann Gletscher
HL 1992
Northing (km)
13
14
15
16
1'7
8
10
12
14
16
18
20
22
Easting (km)
(a)
1992 to 1996 retreat
Northing (km)
0.4
0.2
0.0
−0.2
−0.4
−0.6
8
10
12
14
16
18
20
22
Easting (km)
(b)

Figure 4

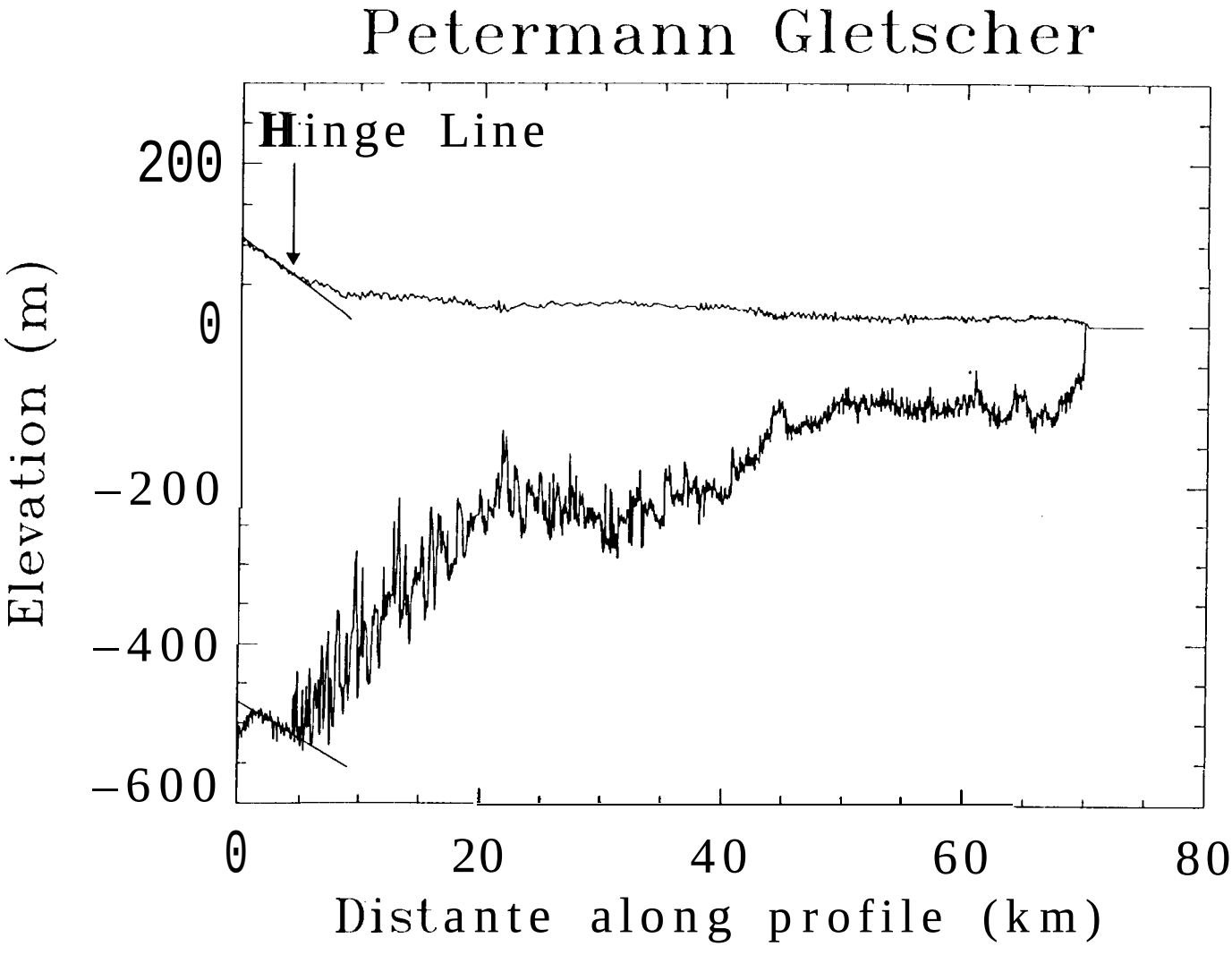
Petermann Gletscher
Hinge Line
200
0
−200
−400
−600
Elevation (m)
0
20
40
60
80
Distante along profile (km)

Figure 5